Healing of Critical-Size Cranial Defects in Guinea Pigs Using a Bovine Bone-Derived Resorbable Membrane

Márcio Luiz de Lima Taga, DDS, MSc[1]/José Mauro Granjeiro, DDS, MSc, PhD[2]/
Tania Mary Cestari, BSc, PhD[3]/Rumio Taga, DDS, MSc, PhD[4]

Purpose: *To investigate the healing of critical-size cranial bone defects (9-mm-diameter) in guinea pigs treated with a bovine bone-derived resorbable membrane.* ***Materials and Methods:*** *A sample of 42 guinea pigs was divided into test (n = 20), control (n = 20), and standard (n = 2) groups. A full-thickness trephine defect was made in the fronto-parietal bone of each animal. In the test group, the internal and external openings of the defect were each closed with a separate membrane, and the space between them was filled with blood clot and a central spacer. In the control group, the defect was filled only with the blood clot and spacer. At 1, 3, 6, and 9 months later, the calvarias (5 per period) for both the test and control groups were collected, fixed, radiographed, and histologically processed. The standard-group animals were sacrificed immediately after surgery and used to determine the initial size of defect radiographically. The areas of defects in the radiographs were measured with image-analysis software and were compared between groups and periods by multiple regression analysis with the Bonferroni correction.* ***Results:*** *At 1 and 3 months, newly formed woven bone was histologically observed in both test and control groups. Radiographically, this new bone occupied an average of 32% of the defect area at 1 month and 60% at 3 months in the test group. In the control group, 21% of the defect was filled at 1 month and 39% at 3 months. However, the differences between treatments were not statistically significant (P > .05). At 6 and 9 months, a significant increase in newly formed lamellar bone was seen histologically in both groups. Radiographically, for the test group, the new bone occupied an average of 82% of the defect area at 6 months and 96% at 9 months. For the control group, new bone composed an average of 45% of the defect area at 6 months and 40% at 9 months. The differences between the test and control groups were statistically significant at 6 and 9 months (P < .05). Complete or almost complete filling of the defect was observed in several cases.* ***Conclusion:*** *It was concluded that the bovine bone-derived membrane is highly biocompatible and is able to promote good healing of critical-size defects in calvaria of guinea pig.* Int J Oral Maxillofac Implants 2008;23:427–436

Key words: *calvaria, collagen, critical-size bone defect, guided bone regeneration, membrane, xenograft*

[1]Graduate Student, Department of Prosthodontics, Bauru Dental School, University of São Paulo, Bauru, SP, Brazil.
[2]Associate Professor, Department of Cell and Molecular Biology, Institute of Biology, Fluminense Federal University (UFF), Niterói, RJ, Brazil.
[3]Graduate Student, Department of Biological Sciences, Bauru Dental School, University of São Paulo, Bauru, SP, Brazil.
[4]Professor, Department of Biological Sciences, Bauru Dental School, University of São Paulo, Bauru, SP, Brazil.

Correspondence to: Prof Dr Rumio Taga, Departamento de Ciências Biológicas, Faculdade de odontologia de Bauru, Universidade de São Paulo, Alameda Octávio Pinheiro Brisolla 9-75, Bauru, São Paulo, Brasil, CEP: 17012-901. E-mail: rumiotag@fob.usp.br

Alveolar ridge resorption after tooth extraction or tooth loss due to disuse, disease, trauma, or pneumatization of the maxillary sinus represents clinical difficulties in implant therapy, often resulting in anatomic anomalies that impair the placement and/or maintenance of titanium endosseous implants.[1]

Guided bone regeneration is one of the surgical techniques most commonly used to maintain or recover the height and thickness of alveolar bone.[2–4] The principle of guided bone regeneration employs a physical barrier or biological membrane to create an adequate environment protected from the invasion of competing, less differentiated, highly proliferative cells from neighboring tissues, thus promoting

a favorable cellular and molecular microenvironment for the regeneration of bone tissue.[5]

The first commercially available membrane consisted of expanded polytetrafluoroethylene (e-PTFE), which has been associated with excellent experimental and clinical results and therefore has been widely used in surgical practice.[6–10] However, it is not resorbable, and a second surgical intervention is therefore required for its removal, which causes discomfort to the patient and can interfere with the ongoing local tissue repair process.[11] This inconvenience encouraged research on the production of resorbable membranes.

Resorbable collagen membranes are frequently used in dental practice, since collagen is a protein naturally present in the periodontium and bone. It possesses chemotactic and platelet-aggregation properties and is naturally resorbed by the organism.[12,13] Collagen membranes yield results that are clinically similar to those obtained with e-PTFE membranes.[13] Resorbable membranes consisting of type I collagen with excellent biological requisites can be obtained from human cortical bone.[14–16] However, the difficulty of obtaining a sufficient amount of preserved human bone from bone banks and its high cost prevent its frequent use in surgical practice.

Recently, a membrane derived from bovine cortical bone, formed basically of highly structured collagen natural fibers, has been introduced to the market for the treatment of periodontal bone lesions or lesions associated with implant therapy. Relatively little data are available regarding the biological action of this membrane and mechanisms of its resorption. Thus, the objective of the present trial was to radiographically and histologically evaluate the capacity of demineralized bovine cortical bone-derived membrane to favor the healing of cranial critical-size defects created in the calvaria of guinea pigs.

MATERIALS AND METHODS

Animals

Forty-two 5-month-old male guinea pigs, weighing about 600 g each, were obtained from the Central Animal House of Bauru Dental School, University of São Paulo (USP). The animals were divided into a test group (n = 20), a control group (n = 20), and a standard group (n = 2). All animals had free access to pelleted chow, grass, vegetables, and water throughout the experiment.

Test Material

In the test group, resorbable Gen-derm membranes (Baumer, Mogi Mirim, SP, Brazil; Ministry of Health approval no. 103.455.00007) were used for the treatment of bone defects. Blocks of demineralized and fully processed bovine cortical bone free of cells, lipids, and immunogenic proteins were used to produce sections 200 to 300 μm thick, which were freeze-dried.

Scanning Electron Microscopy Characterization of the Membrane

Microstructural analysis of the membrane was performed at the Núcleo de Apoio à Pesquisa em Microscopia Eletrônica Aplicada à Pesquisa Agropecuária (NAP/MEPA), ESALQ, USP. Ten fragments with a surface area of 25 mm^2 were sputtered with 100 to 200 Å gold in a Balzers MED 010 apparatus (Brügg, Switzerland) and examined in a Zeiss DMS 910A scanning electron microscope (Carl Zeiss, Oberkochen, Baden-Württemberg, Germany). The images were captured with DITI software (Carl Zeiss) and stored in Windows bitmap (bmp) format. The membrane surface microstructure and the number and size of its pores were determined on electron photomicrographs.

Surgical Procedures

The experimental methodology was approved and conducted according to the guidelines for laboratory animal experimentation of Bauru Dental School, USP.

A schematic drawing of the experimental model is presented in Fig 1. General anesthesia was attained via intramuscular injection of ketamine (0.35 mL/kg; Parke-Davis/Achë Laboratórios Farmacêuticos, Guarulhos, SP, Brazil) and xylazine (0.25 mL/kg; Bayer, São Paulo, SP, Brazil) followed by fronto-parietal trichotomy and vigorous asepsis with an alcoholic iodine solution. A half-moon incision was made in the fronto-parietal tegument with a no. 10 surgical blade, and the flap was elevated posteriorly with a Molt elevator and an Ochsenbein no. 1 chisel, exposing the cranial bone surface. Next, a full-thickness defect was made with a surgical trephine (9-mm outer diameter) under abundant and continuous irrigation with physiologic saline solution. In the test group, 1 Gen-derm membrane was placed above the dura mater to close the internal opening of the defect, and the second was placed on the external opening. The defect space between membranes was filled with the blood clot and a central spacer (Fig 1). A rod spacer of 3 × 4 × 3 mm was used to maintain the defect space between the membranes; this spacer was obtained from 0.6 mol/L HCl-demineralized allogeneic parietal bone treated with 4 mol/L guanidine hydrochloride for deactivation of its osteoinductive potential.[16] In the control and standard groups, the defect was only filled with the blood clot and spacer (Fig 1). The flaps were closed with 3-0 black silk suture (Johnson & Johnson/Ethicon, Somerville, NJ).

Histologic Procedures

The guinea pigs (5 animals/period) of the control and test groups were sacrificed at 1, 3, 6, and 9 months after surgery by an overdose of anesthetics. Two animals of the standard group were killed 0 h after surgery and were used to determine the initial size of defects. The calvarias were then collected and fixed in 10% phosphate-buffered formalin (pH 7.3) for 1 week. Radiographs of the calvarias were then obtained. After demineralization in Morse solution[17] (30% formic acid and 20% sodium citrate) for 6 weeks, the specimens were dehydrated in ethanol, cleared in xylene, and embedded in Histosec (Merck, Darmstadt, Germany). Five-µm-thick sections of each whole defect were obtained at 200-µm intervals. Cuts were made in a laterolateral direction, and the sections were stained with hematoxylin-eosin. About 40 to 50 sections per specimen were used in the histologic analysis.

Radiographic Quantitative Analysis

Radiographic images obtained on optical plates at 70 kVp, 10 mA, focus-film distance of 40 cm and exposure time of 0.26 second were transferred to the Kontron KS300 digital image analysis system (Kontron Elektronik, Image Analysis Division, Eching, Munich, Germany). A program was designed for automatic measurements. First, the initial area of the defect (A_i) was measured in the standard group at 0 h. The radiolucent area of the defect, ie, the area without bone tissue formation (A_{luc}), was determined at the other time periods in the test and control groups. The area of the defect filled with newly formed bone (A_{bone}) was calculated for each animal using the following equation: $A_{bone} = A_i - A_{luc}$.

Statistical Analysis

Data of defect areas (A_{luc}) from the control and experimental groups were compared between groups and periods by multiple regression analysis with the Bonferroni correction by using R software (The R Foundation for Statistical Computing, Institut für Statistik und Wahrscheinlichkeitstheorie, Technische Universität Wien, Vienna, Austria).

RESULTS

Postoperative follow-up showed no signs of infection in the surgical area in any guinea pig. Some animals presented small edemas that disappeared completely within a few days, with no suppuration or opening of the incision.

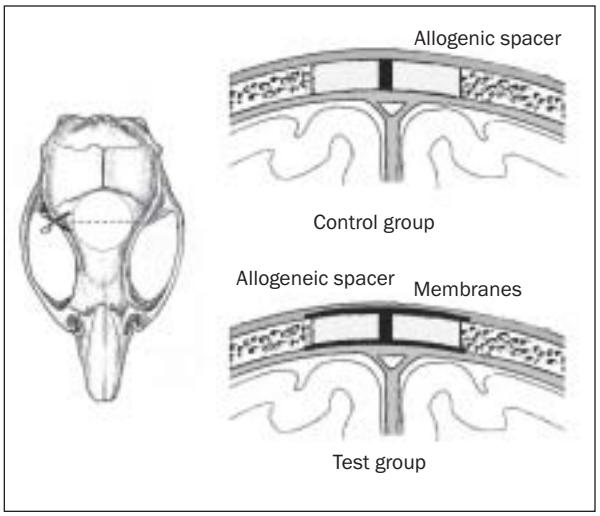

Fig 1 Schematic drawing of the experimental model. Two membranes were used for each test-group defect.

Scanning Electron Microscopy Analysis

Scanning electron microscopy (SEM) analysis (Fig 2) revealed that the membrane exhibited homogenously distributed pores and a slightly undulated surface with lines and bundles, delimiting the arrangement of more superficial collagen fibers. The small pores corresponded to osteocyte lacunae. They had a mean diameter of 10 µm, and approximately 3/mm^2 were observed. The large pores, corresponding to haversian and Volkmann canals, had a mean diameter of 62 µm; about 12/mm^2 were observed.

Descriptive and Quantitative Radiographic Results

The most representative radiographic images of events observed at 0 h, control and test groups are presented in Figs 3 and 4. Table 1 shows the results regarding area of the defects in mm^2. The estimated curves correlating the area of the defect and time obtained by multiple regression analysis are illustrated in Fig 5. The differences between measurements obtained after Bonferroni correction and the respective levels of probability of observed differences are shown in Table 2.

The mean area of the defect immediately after surgery (Fig 3a) was 66.3 mm^2. At 1 month, newly formed bone was observed along the lateral and posterior borders of the defect in both the control (Fig 3b) and test groups (Fig 4a), reducing the mean area of the defect to 52.2 mm^2 (21%) and 45.3 mm^2 (32%), respectively. The difference between treat-

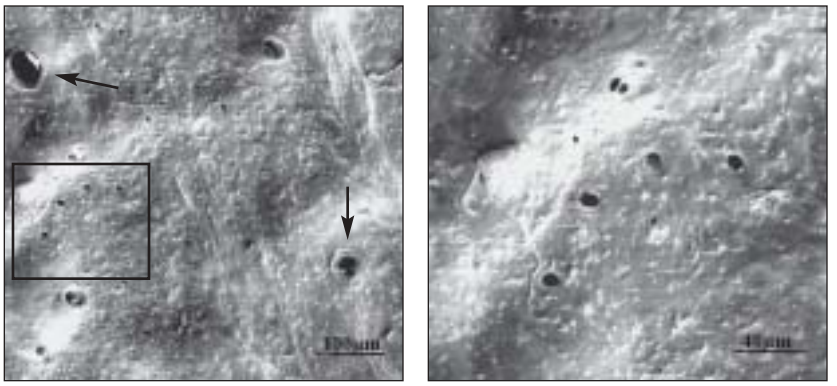

Fig 2 Scanning electron photomicrograph of a membrane. *(a)* Several small pores *(boxed area)* and large pores *(arrows)* on the membrane surface. *(b)* Detail of the small pores.

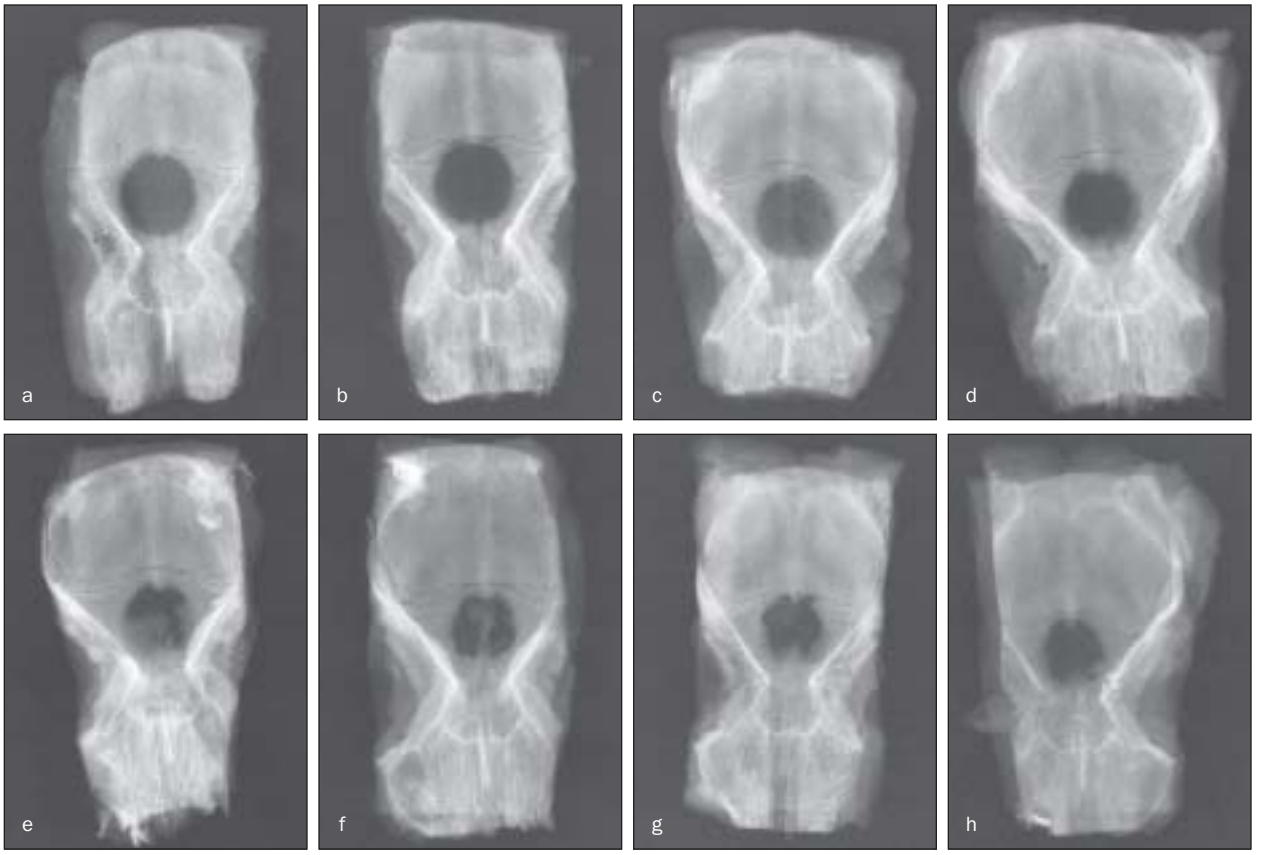

Fig 3 Radiographic images of the control group at *(a)* 0 hour, *(b and c)* 1 month, *(d)* 3 months, *(e and f)* 6 months, and *(g and h)* 9 months.

ments after Bonferroni correction (Table 2) was not statistically significant ($P > .05$). Greater bone formation with significant reduction in defect opening was observed in 1 control animal (Fig 3c) and 2 animals from the test group (Fig 4b).

At 3 months, the amount of newly formed bone along the borders of the defect had increased in both the control (Fig 3d) and test (Fig 4c) groups. New bone formation was markedly higher in 3 specimens of the test group compared to the control defects. One test case showed almost complete closure of the defect (Fig 4d). Thus, compared to the 0 h group, the area of the defects decreased 39% and 60% for the control and test groups, respectively, with mean areas measuring 40.7 mm^2 and 26.6 mm^2, respectively (Table 1). However, the difference observed between treatments was not statistically significant (Table 2).

At 6 months, it was observed that the continuity of new bone formation along the borders of defects resulted in mean closures of 55% and 82% of the original defects in the control and test groups, respectively,

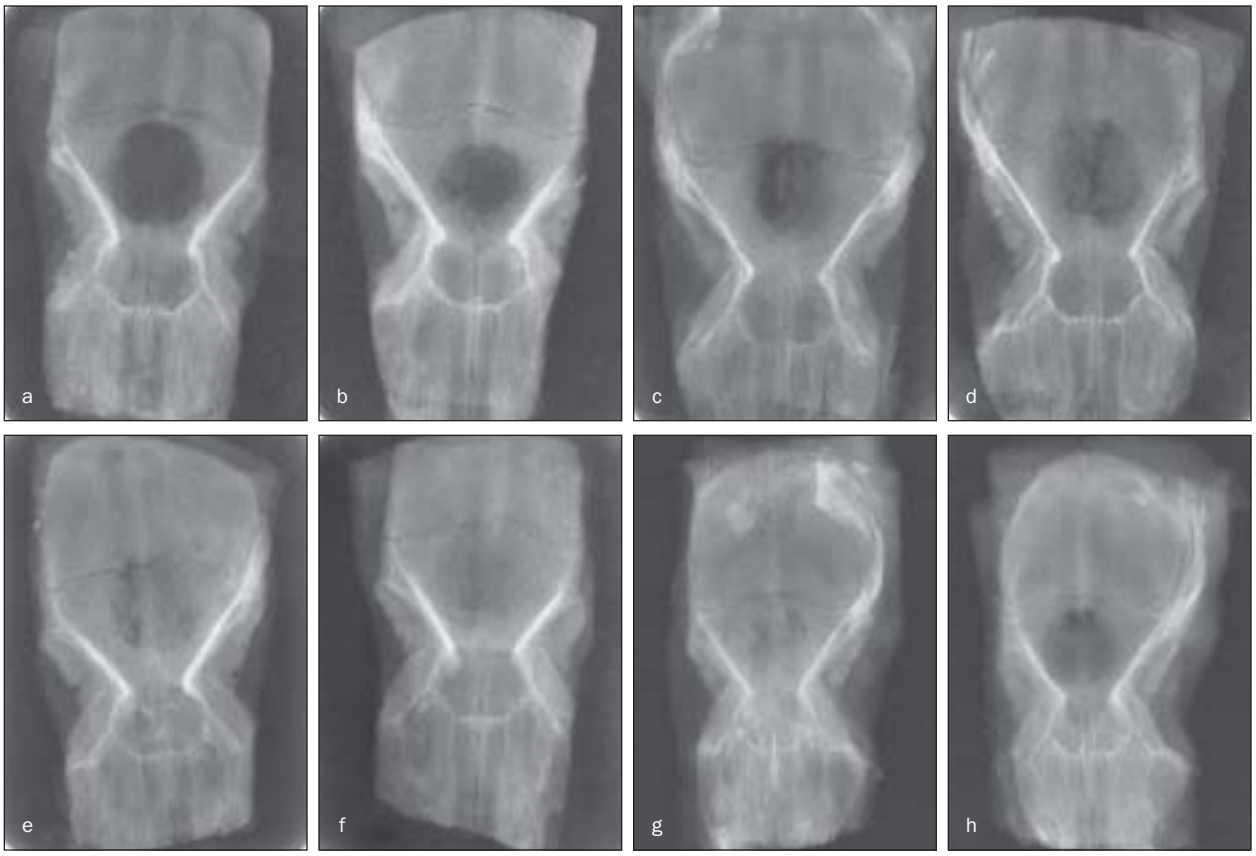

Fig 4 Radiographic images of the test group at *(a and b)* 1 month, *(c and d)* 3 months, *(e and f)* 6 months, and *(g and h)* 9 months.

with mean areas of 29.6 mm^2 and 12.0 mm^2, respectively. Nearly complete closure was observed in 2 test group specimens (Figs 4e and 4f), and slight bone formation occurred in 1 case. All animals of the control group showed increased closure along the entire circumference of the defect. However, greater bone formation was observed in 2 cases—in the anterior half in one case (Fig 3e) and in the region of the median suture in the other (Fig 3f). In this period, the 146% difference in the mean area between control and test groups was statistically significant (Table 2, $P < .05$).

At 9 months, the opening of control defects had increased compared to the previous period, probably due to bone remodeling (Figs 3g and 3h). In the test group, complete closure was observed in 1 defect (Fig 4g), and almost complete closure was observed in the other 2 defects (Fig 4h). The decrease in the area of defects was 45% in the control group and 96% in the test group, with mean areas of 39.6 mm^2 and 2.5 mm^2, respectively. Statistical analysis revealed significant difference (Table 2, $P < .05$) between treatments.

Table 1 Radiolucent Area of the Defects in mm^2

Group/ time (mo)	n	Mean	SD
Standard			
0 h	2	66.3	0.2
Control			
1	5	52.2	7.1
3	5	40.7	11.9
6	5	29.6	14.0
9	5	36.2	7.3
Total	20	39.6	12.8
Experimental			
1	5	45.3	16.4
3	5	26.6	11.3
6	5	12.0	9.5
9	5	2.5	1.7
Total	20	21.6	19.4

Histologic Results

Test Group. One month after surgery (Fig 6), 2 animals of the test group presented an almost intact membrane in both the external and internal openings. The external membrane was surrounded by richly cellularized and vascularized connective tissue with mononucleated cells and blood remnants, which also occupied its canals and pores. The internal membrane was surrounded by newly formed woven bone intimately associated with its surface (Figs 6b and 6d).

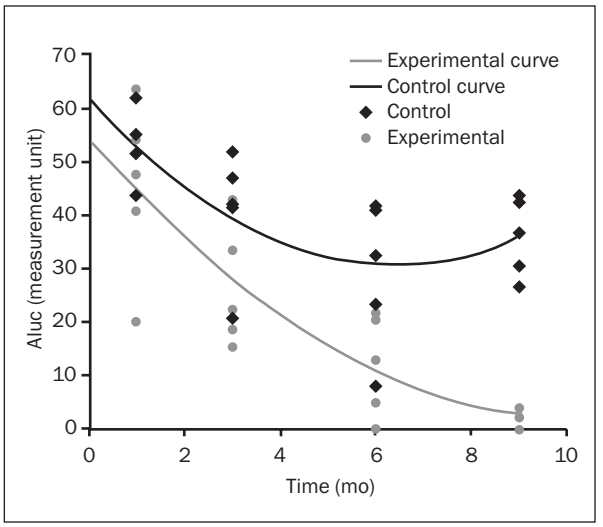

Table 2 Comparison and 95% Confidence Interval of the Mean Differences Between Groups for Each Period

Time (mo)	Mean estimated diference (control vs experimental)	Confidence Interval of the 95%	
		Lower limit	Upper limit
1	8.13	−8.47	24.73
3	11.23	−0.87	23.34
6*	19.78	5.47	34.09
9*	32.98	15.71	50.25

*$P < .05$.
Multiple Regression Analysis with Bonferroni Correction)

Fig 5 Estimated curves correlating the area of the defect and time, obtained by multiple regression analysis.

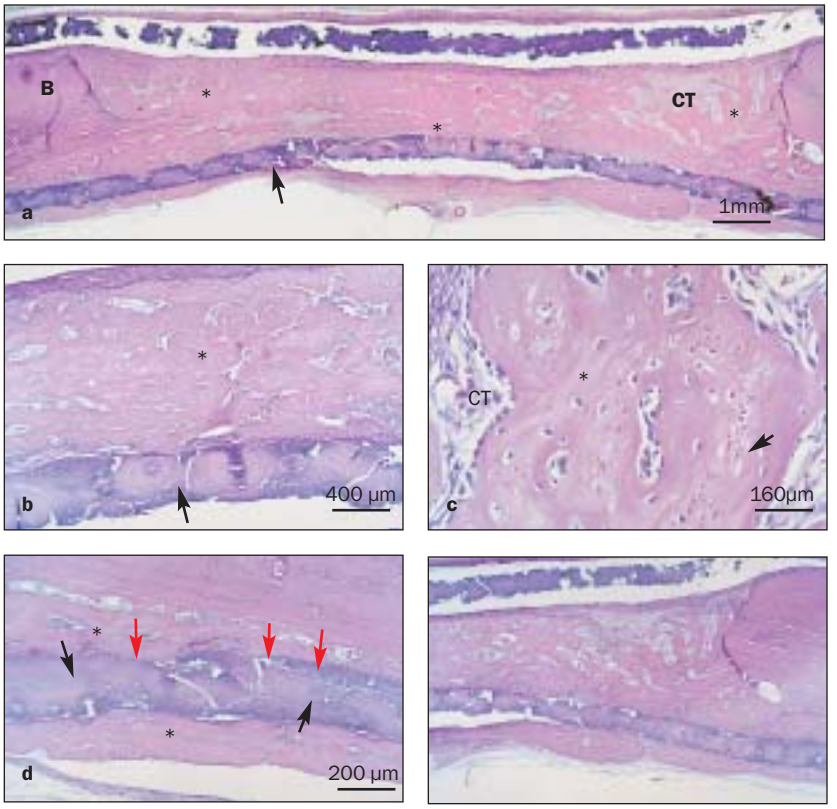

Fig 6 Test group, 1 month. Observe *(a)* borders of the defect (B), bone defect filled with new bone *(asterisks)*, connective tissue (CT), external and internal membranes *(black arrows)*; *(b)* intact internal membrane *(black arrows)* associated with the newly formed bone *(asterisks)*; *(c)* erythrocytes *(black arrow)* inclued in the new bone *(asterisks)* and *(d)* direct bone formation apposed to the internal membrane *(black arrows)* and surface *(red arrows)* (hematoxylin-eosin).

Nevertheless, in 3 animals, the membranes were completely or partially resorbed by mononucleated cells, with slight new bone formation on the membrane surface (Fig 6a). No inflammatory infiltrate was observed in any specimen. Intense new bone formation was observed inside the defect from the bone border to the central region, where the spacer was undergoing resorption. In 2 cases, newly formed woven bone occupied almost the entire defect space. Blood clot remnants trapped inside the newly formed bone matrix were noted (Fig 6c).

At 3 months (Fig 7), the external membrane was undergoing resorption (Figs 7a and 7b), whereas the internal membrane was well resorbed, with remnants trapped inside the newly formed bone (Figs 7c and 7d). The defect was filled with new bone tissue, which formed compact fused bone islands or was separated by a thin layer of connective tissue (Figs 7a and 7b). In the central region of the defect (Fig 7a), the spacer was already well resorbed and surrounded by bone tissue and/or fibrous connective tissue. The limits of the bone border were clearly visible but were already

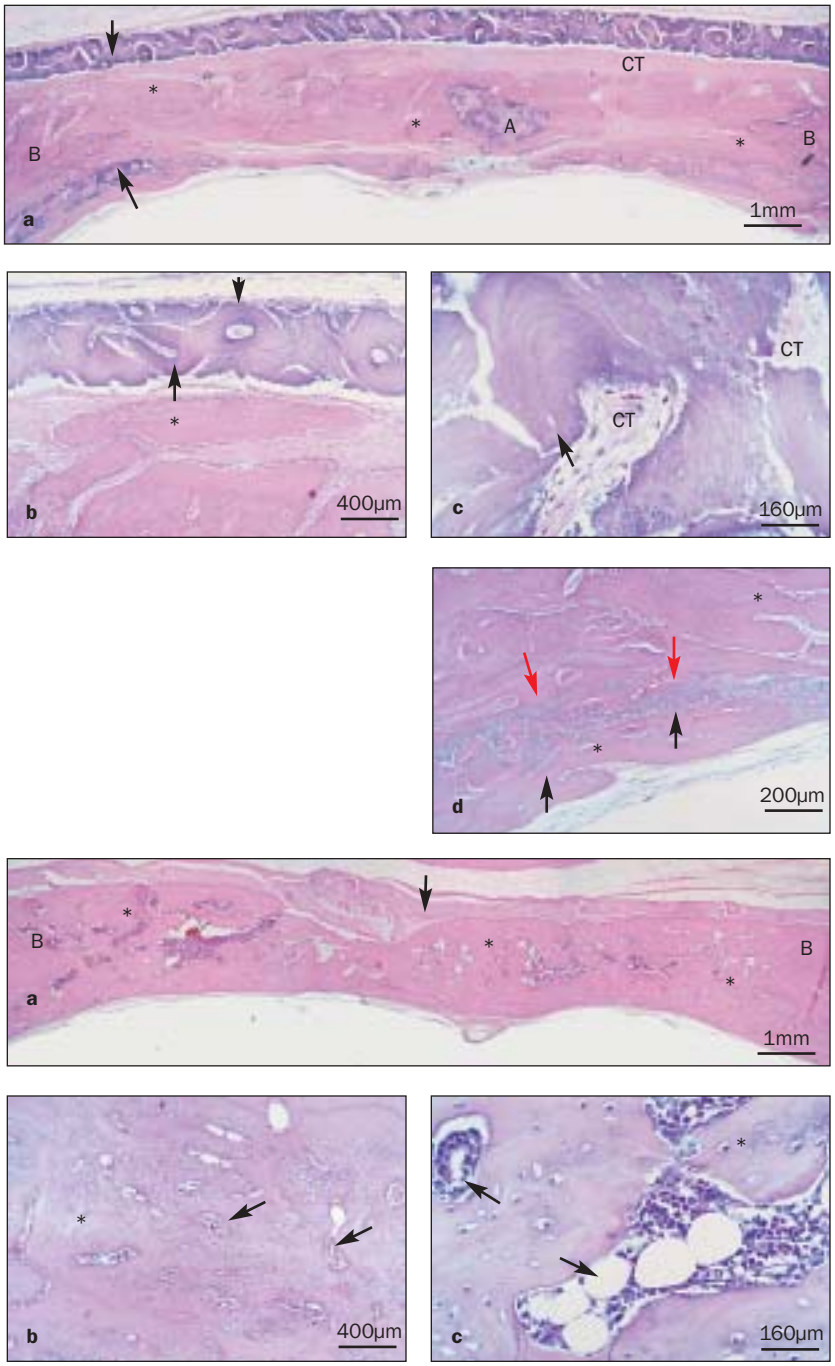

Fig 7 Test group, 3 months. Observe: *(a)* borders of the defect (B), defect filled with newly formed bone islands *(asterisk)*, connective tissue (CT) and block of allogeneic bone (A), intact external membrane *(top black arrow)*, and internal membrane *(bottom black arrow)* undergoing resorption, with their fragments included in the newly formed bone *(asterisks)*; *(b)* intact external membrane *(arrows)* and bone islands *(asterisk)* involved by connective tissue (CT); *(c)* fragments of membrane *(black arrow)* included in the newly formed bone; and (d) bone formation *(asterisks)* directly apposed to the membrane surface *(red arrows)* (hematoxylin-eosin).

Fig 8 Test group, 6 months. Observe *(a)* borders of the defect (B), defect filled with newly formed bone *(asterisks)*, and external membrane *(black arrow)* partially resorbed; *(b and c)* newly formed bone *(asterisk)* and red bone marrow *(arrows)* (hematoxylin-eosin).

undergoing remodeling and fusion with the newly formed bone tissue that filled the defect (Fig 7a).

At 6 months (Fig 8), the external membrane was still intact or partially resorbed (Fig 8a), while the internal membrane was absent or almost completely resorbed. The defect was completely filled with lamellar bone tissue and bone marrow (Figs 8b and 8c) or with large bone islands containing bone marrow. No bone tissue formation was observed in 1 specimen, whose defect was filled with connective tissue.

At the end of 9 months (Fig 9), complete closure of the defect was observed in 3 cases (Fig 9a) and almost complete closure was observed in the other 2 cases. Either new bone continuously filled the entire defect (Figs 9b and 9c) or the defect space was completely filled with fused bone islands or islands separated by connective tissue bands or adipose tissue.

Control Group. No marked difference in histologic features was observed for the control group at any time point (Fig 10). In this respect, formation of bone tissue occurred from the borders of the defect, and the remaining defect was filled with fibrous connective tissue (Fig 10). In some cases, the formation of a thin bone tissue band, which probably replaced the spacer, was observed in the region of the median suture.

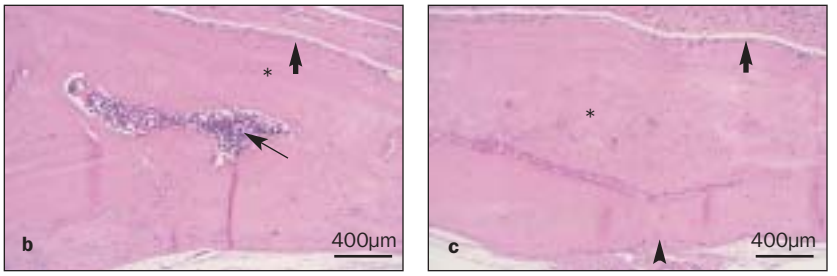

Fig 9 Test group at 9 months. *(a)* The borders of the defect (B). The defect was filled with compact bone (*) and bone marrow *(arrows)* already showing similarity with the original bone. *(b)* Newly formed bone (*) and red bone marrow *(thin arrow)* in the defect border covered with periosteum *(thick arrow)*. *(c)* Compact bone (*) in the center of the defect covered with periosteum *(thick arrow)*. Note the suture line formation *(arrowhead)* (hematoxylin-eosin).

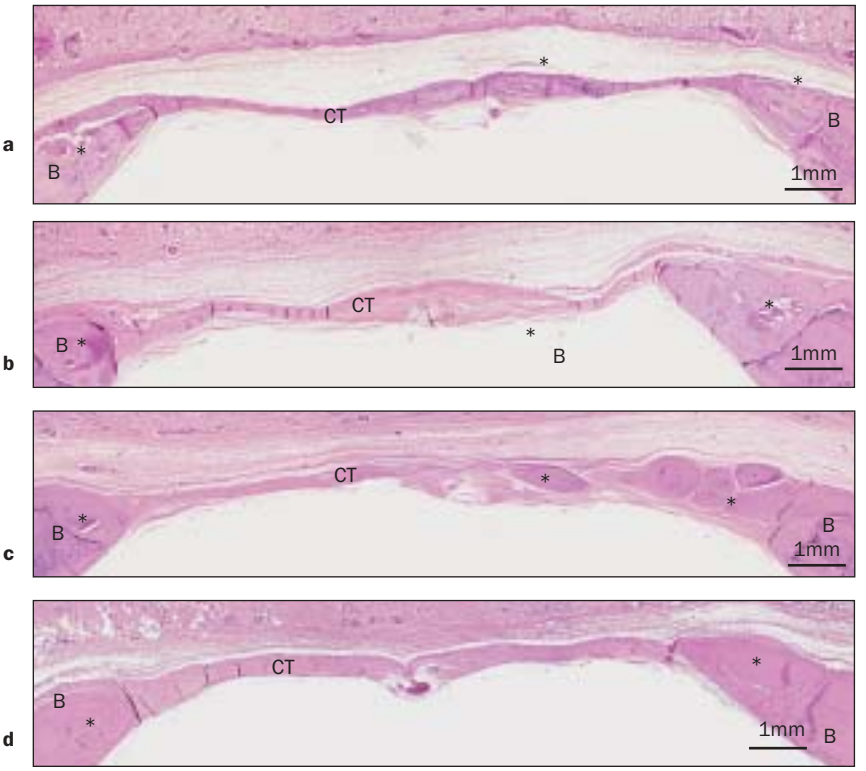

Fig 10 Control group at *(a)* 1 month, *(b)* 3 months, *(c)* 6 months, and *(d)* 9 months. B = defect border. Observe *(a and b)* slight bone formation (*) at the borders and in the central regions of the defect and *(c and d)* slight new bone formation (*) at the defect border and in the defect space along with connective tissue (CT).

DISCUSSION

In the present study, the bone-healing capacity of a membrane produced with demineralized bovine cortical bone treated for inactivation of potential matrix antigens was evaluated in critical-size defects created in the skulls of guinea pigs. According to the manufacturer, the membrane is resorbable and basically consists of highly structured collagen I, with the natural canals and pores of a long cortical bone.

Various studies have demonstrated the high efficiency and biocompatibility of collagen membranes in healing bone defects by guided tissue regeneration in both animal[13,18–25] and human models.[12,26–31] Structured collagen bone matrix serves as an ideal substrate for recruitment and anchorage of progenitor cells and consequently for the proliferation and terminal differentiation of osteoblasts; it also acts as a carrier and protector of bone morphogenetic proteins against nonspecific proteolytic enzymes.[31]

In no control-group animal was the 9-mm defect filled with bone tissue at any of the 4 time points. In all cases, formation and invagination of dense connective tissue into the defect were noted, irrespective of the study period, with formation of bone tissue only at the borders of the defect, as has been reported by others.[23,33–35] These results confirmed that the 9-mm defect created in calvarias of guinea pigs is a critical-size

defect,[36] ie, spontaneous regeneration does not occur when the defect is filled only with a blood clot, even after 9 months. In some cases, slight new bone formation was observed in the region of the median suture of the parietal bone, probably because of the presence of the inactive demineralized allogeneic bone spacer.

The radiographic and histologic results obtained for the test group showed that the use of 2 bovine cortical bone membranes, together with a spacer, favored bone regeneration in critical-size defects created in the calvarias of guinea pigs, with complete or almost complete filling of the defect after 6 to 9 months of treatment. Histologically, complete filling of the defect with primary woven and poorly mineralized bone, which is sometimes not detectable on radiographs, was observed in some specimens as early as 1 month after surgery. This initial osteogenesis was so intense and rapid that fragments of blood clot were incorporated into the newly formed bone matrix.

An interesting observation in some specimens was the direct deposition of bone tissue on the surface of the internal membrane, which caused its incorporation into the newly formed bone and increased bone thickness in the region, especially close to the border of the defect, a finding less frequently noted for the external membrane. This observation, together with the absence of inflammatory infiltrate close to the membranes at all time points studied, suggest that the membrane has osteoconductive properties.

In some cases, as reported by other investigators,[33–35] the presence of highly vascularized bone marrow close to the newly formed bone and a structure resembling the sagittal suture located in the lower central part of the defect was noted as early as 1 month after surgery, but the thickness of new bone in these cases was still smaller than that of the original calvaria bone.

At 6 and 9 months, the new bone consisted of a combination of compact and cancellous bone, with small fragments of membrane incorporated into the remodeling bone. In some cases, at 9 months, the formed cortical plate started to present the morphology of the original calvaria bone.

In all cases new bone formation occurred by intramembranous ossification. In contrast, Sandberg et al[3] observed endochondral ossification in rat cranial defects treated with resorbable polylactic/polyglycolic acid copolymer membranes. According to these authors, this type of ossification may have occurred due to low oxygenation resulting from impaired gaseous diffusion through the membranes used. The differences in the results of the investigations suggest that the present membrane does not show this difficulty, probably because of the presence of natural pores.

Despite the use of a spacer, collapse of the membrane inside the defect was observed in some specimens, probably because of more rapid resorption of the external barrier. This impaired new bone formation in the region in these cases, a finding that might explain the decreased bone formation observed in some specimens at 3 and 6 months after surgery. A similar collapsing effect was reported by Linde et al[4] with utilization of e-PTFE membranes.

Comparison of the present parametric results showed similar bone formation in the control and experimental groups up to 3 months after surgery. At subsequent time points, bone tissue deposition was drastically reduced in the control group, with stabilization of the size of the bone defect, whereas in the experimental group new bone formation continued, following the same pattern as previously observed, ie, a gradual decrease in the size of the defect until complete or almost complete closure in most cases. After 9 months, the mean bone gain compared to the original defect was 96% for the experimental group and 45% for the control group, a statistically significant difference. Comparatively, Ito et al[37] reported recovery rates of 89.0% for an e-PTFE membrane and 54.7% for a polylactic acid membrane in rabbit calvarias after 6 months.

While the bovine cortical bone-derived membrane remained functional, it was resorbed more slowly than other collagen membranes have reportedly been resorbed.[25] This longer persistence of the present bovine bone-derived membrane is probably related to crosslinks naturally present in the material, suggesting that the inclusion of artificial crosslinks to increase its resistance to resorption is not necessary. Membrane fragments were observed even at 9 months postoperatively. Membranes showing some structural integrity were present in various animals at 3 months after placement. In most animals, the defect was almost completely filled with woven bone as early as after 1 month of treatment. Evidence suggests that maintenance of its integrity for 1 to 3 months is sufficient for the membrane to exert its soft tissue exclusionary function, protecting the blood clot, preventing defect invasion by highly proliferating neighboring nonosseous connective tissue. The membrane is able to create a favorable molecular and cellular environment for the proliferation and migration of osteoprogenitor cells, their maturation into osteoblasts, and extremely rapid deposition of immature or primary bone matrix throughout the defect space.

Based on the present results, it was concluded that the biological membrane derived from bovine cortical bone is highly biocompatible and has a high capacity to favor bone healing in cranial critical-size defects, remaining functional for a sufficient period to allow bone regeneration. In addition, this membrane possesses osteoconductive properties that permit the formation of new bone on its surface.

ACKNOWLEDGMENTS

This research was supported by CNPq (grant no. 551831/2002-2) and by FAPESP (grant no. 00/00877-0).

REFERENCES

1. Linde A, Alberius P, Dahlin C, Bjurstam K, Sundin Y. Osteopromotion: A soft-tissue exclusion principle using a membrane for bone healing and bone neogenesis. J Periodontol 1993; 64(suppl):1116–1128.
2. Zellin G, Linde A. Effects of different osteopromotive membrane porosities on experimental bone neogenesis in rats. Biomaterials 1996;17:695–702.
3. Sandberg E, Dahlin C, Linde A. Bone regeneration by the osteopromotion technique using bioabsorbable membranes: An experimental study in rats. J Oral Maxillofac Surg 1993;51: 1106–1114.
4. Linde A, Thorén C, Dahlin C, Sandberg E. Creation of new bone by an osteopromotive membrane technique: An experimental study in rats. J Oral Maxillofac Surg 1993;51:892–897.
5. Nyman S, Karring T, Lindhe J, Planten S. Healing following implantation of periodontitis affected roots into gingival connective tissue. J Clin Periodontol 1980;7:394–401.
6. Tinti C, Vincenzi G, Cocchetto R. Guided tissue regeneration in mucogingival surgery. J Periodontol 1993;64(suppl):1184–1191.
7. Becker W, Becker BE. Treatment of mandibular 3-wall intrabony defects by flap debridement and expanded polytetrafluoroethylene barrier membranes. Long-term evaluation of 32 treated patients. J Periodontol 1993;64(suppl):1138–1144.
8. Cortellini P, Tonetti MS. Focus on intrabony defects: Guided tissue regeneration. Periodontol 2000 2000;22:104–132.
9. Karring T, Cortellini P. Regenerative therapy: Furcation defects. Periodontol 2000 1999;19:115–137.
10. Wang H-L, Caroll WJ. Guided bone regeneration using bone grafts and collagen membranes. Quintessence Int 2001;32:504–515.
11. Scott TA, Towle HJ, Assad DA, Nicoll BK. Comparison of bioabsorbable laminar bone membrane and non-resorbable ePTFE membrane in mandibular furcations. J Periodontol 1997;68:679–686.
12. Wang HL, Macneil RL. Guided tissue regeneration. Absorbable barriers. Dent Clin North Am 1998;42:505–522.
13. Bunyaratavej P, Wang HL. Collagen membranes: A review. J Periodontol 2001;72:215–229.
14. Silverstein LH, Kraft JD, Wand R. Bone regeneration and tissue acceptance of human fascia lata grafts adjacent to dental implants: A preliminary case report. J Oral Implantol 1992; 18:394–398.
15. Callan DP. Guided tissue regeneration without a stage 2 surgical procedure. Int J Periodontics Restorative Dent 1993;13:172–179.
16. Yamaoka SP, Mellonig JT, Meffert RN, Arnold RM, Nummikoski PV, Mealey BL. Clinical evaluation of demineralized-unicortical-illium-strips for guided tissue regeneration. J Periodontol 1996;67:803–815.
17. Morse A. Formic acid-sodium citrate decalcification and butyl alcohol dehydration of teeth and bones for sectioning in paraffin. J Dent Res 1945;24:143–153.
18. Pitaru S, Tal HA, Soldinger M, Grosskopf A, Noff M. Partial regeneration of periodontal tissues using collagen barriers. Initial observations in the canine. J Periodontol 1988;59: 380–386.
19. Colangelo P, Piattelli A, Barrucci S, Trisi P, Formisano G, Caiazza S. Bone regeneration guided by resorbable collagen membranes in rabbits: A pilot study. Implant Dent 1993;2:101–105.
20. Sevor JJ, Meffert RM, Cassingham RJ. Regeneration of dehisced alveolar bone adjacent to endosseous dental implants utilizing a resorbable collagen membrane: Clinical and histologic results. Int J Periodontics Restorative Dent 1993;13:71–83.
21. Hürzeler MB, Kohal RJ, Naghshbandi J, et al. Evaluation of a new bioresorbable barrier to facilitate guided bone regeneration around exposed implant threads. An experimental study in the monkey. Int J Oral Maxillofac Surg 1998;27:315–320.
22. McGinnis M, Larsen P, Milor M, Beck FM. Comparison of resorbable and nonresorbable guided bone regeneration materials: A preliminary study. Int J Oral Maxillofac Implants 1998;13:30–35.
23. Zahedi S, Legrand R, Brunel G, et al. Evaluation of a diphenylphosphorylazide-crosslinked collagen membrane for guided bone regeneration in mandibular defects in rats. J Periodontol 1998;69:1238–1246.
24. Hockers T, Abensur D, Valentini P, Legrand R, Hämmerle CH. The combined use of bioresorbable membranes and xenografts or autografts in the treatment of bone defects around implants. A study in beagle dogs. Clin Oral Implants Res 1999;10:487–498.
25. Owens KW, Yukna RA. Collagen membrane resorption in dogs: A comparative study. Implant Dent 2001;10:49–58.
26. Zitzmann NU, Naef R, Scharer P. Resorbable versus nonresorbable membranes in combination with Bio-Oss for guided bone regeneration. Int J Oral Maxillofac Implants 1997;12: 844–852 [erratum 1998;13:576].
27. Parodi R, Carusi G, Santarelli G, Nanni F. Implant placement in large edentulous ridges expanded by GBR using a bioresorbable collagen membrane. Int J Periodontics Restorative Dent 1998;18:266–275.
28. Benque E, Zahedi S, Brocard D, Marin P, Brunel G, Elharar F. Tomodensitometric and histologic evaluation of the combined use of a collagen membrane and a hydroxyapatite spacer for guided bone regeneration: A clinical report. Int J Oral Maxillofac Implants 1999;14:258–264.
29. Cortellini P, Tonetti MS. Focus on intrabony defects: Guided tissue regeneration. Periodontol 2000 2000;22:104–132.
30. Brunel G, Brocard D, Duffort JF, et al. Bioabsorbable materials for guided bone regeneration prior to implant placement and 7-year follow-up: Report of 14 cases. J Periodontol 2001;72: 257–264.
31. Zitzmann NU, Scharer P, Marinello CP. Long-term results of implants treated with guided bone regeneration: A 5-year prospective study. Int J Oral Maxillofac Implants 2001;16: 355–366.
32. Ripamonti U, Reddi AH. Periodontal regeneration: Potential role of bone morphogenetic proteins. J Periodontal Res 1994; 29:225–235.
33. Stal S, Tjelmeland K, Hicks J, Bhatia N, Eppley B, Hollier M. Compartmentalized bone regeneration of cranial defects with biodegradable barriers: An animal model. J Craniofac Surg 2001;12:41–47.
34. Dupoirieux L, Pourquier D, Picot MC, Neves M. Comparative study of three different membranes for guided bone regeneration of rat cranial defects. Int J Oral Maxillofac Surg 2001;30: 58–62.
35. Mardas N, Kostopoulos L, Karring T. Bone and suture regeneration in calvarial defects by e-PTFE-membranes and demineralized bone matrix and the impact on calvarial growth: An experimental study in the rat. J Craniofac Surg 2002;13: 453–462.
36. Schmitz JP, Hollinger JO. The critical size defect as an experimental model for craniomandibulofacial nonunions. Clin Orthop 1986;205:299–308.
37. Ito K, Nanba K, Murai S. Effects of bioabsorbable and nonresorbable barrier membranes on bone augmentation in rabbit calvaria. J Periodontol 1998;69:1229–1237.